Advances in Science and Technology Research Journal

Advances in Science and Technology Research Journal 2024, 18(4), 400–409
https://doi.org/10.12913/22998624/189549
ISSN 2299-8624, License CC-BY 4.0

Received: 2024.05.10
Accepted: 2024.06.11
Published: 2024.06.20

Numerical Analysis of Selected Variants of Reinforcements of Thin-Walled Open Load-Bearing Structures Subjected to Torsion

Tomasz Kopecki[1*]

[1] Department or Mechanical Engineering and Aviation, Rzeszów University of Technology, Al. Powstańców Warszawy 8, 35-959 Rzeszów, Poland
E-mail: tkopecki@prz.edu.pl

ABSTRACT

The study concerns the comparative analysis of selected solutions of thin-walled structures subjected to constrained torsion, representing the simulation of wing areas weakened by large cutouts. The chosen variants of stiffening were based on the concept of so-called "Misztal torsion box", used in the wing of the PZL-37 aircraft. A series of numerical analyses were conducted, aiming to compare selected variants of structures with reinforcements and a reference structure based on a traditional design scheme. The calculations were performed using software based on the finite element method. An analysis of the stress and displacement distribution of the examined structure was conducted, and the results demonstrating the advantages of the proposed structural solution were presented.

Keywords: thin-walled structures, torsion, finite element method, stability loss, critical load.

INTRODUCTION

Contemporary aircraft load-bearing structures, due to the necessity of meeting requirements regarding weight limits, strength, and ensuring appropriate aerodynamic properties, are predominantly based on the utilization of surface-mounted thin-walled structures. This necessitates consideration of the possibility of encountering the phenomenon of stability loss, which in the case of certain aircraft components is permissible within a local and elastic range.

The stability loss effect most commonly occurs in the case of surface structures subjected to torsion, such as the working covers of semi-monocoque structures. This phenomenon is particularly detrimental in the case of critical components whose function is to provide the required torsional rigidity to the structure. In such cases, it is entirely unacceptable. For example, in the case of the wing torsion box, eliminating the possibility of stability loss of the cover is required. Another example can be found in aircraft fuselage areas where large cutouts occur due to operational reasons. Areas of this type include, for example, door openings, baggage compartments, windows, and inspection openings. In all mentioned cases, the standard solution ensuring adequate structural rigidity is the use of framing. A significantly more demanding type of cutout, essentially reducing the torsional stiffness of the aircraft fuselage, is the open cockpit area, exposed to strong torsional loads in some types of aircraft structures (Fig.1). In such solutions, most commonly used in light, aerobatic, and training aircraft, the transparent cockpit canopy serves solely aerodynamic functions and provides comfort to the crew, but does not constitute a stiffening element of the cutout perimeter. The main cause of torsional loads is the forces resulting from asymmetric gusts (horizontal stabilizer) and forces generated by the vertical stabilizer during control. From a strength point of view, the presence of a cutout in such a form means the occurrence of a section of the fuselage with an open circumference, adjacent to areas with closed circumferences, which can be illustrated by a simplified model (Fig. 2a). Since a thin-walled profile with an open circumference exhibits practically zero torsional stiffness, it is necessary to apply

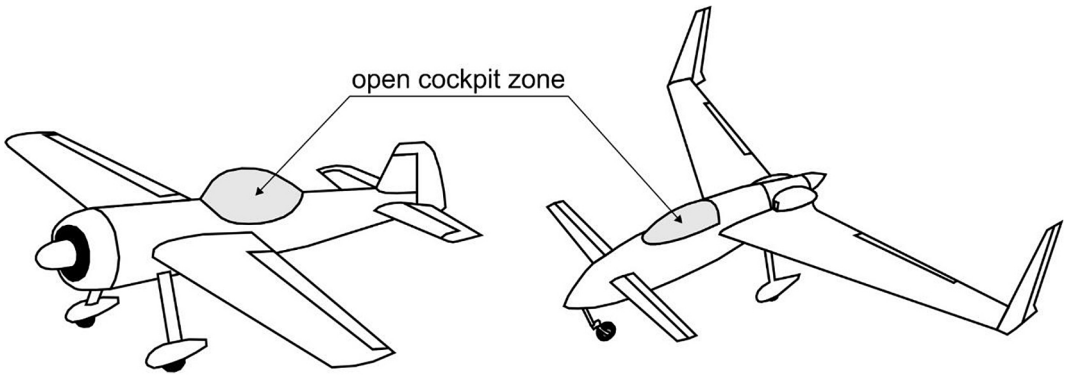

Figure 1. Examples of the large cutout in the cockpit zone

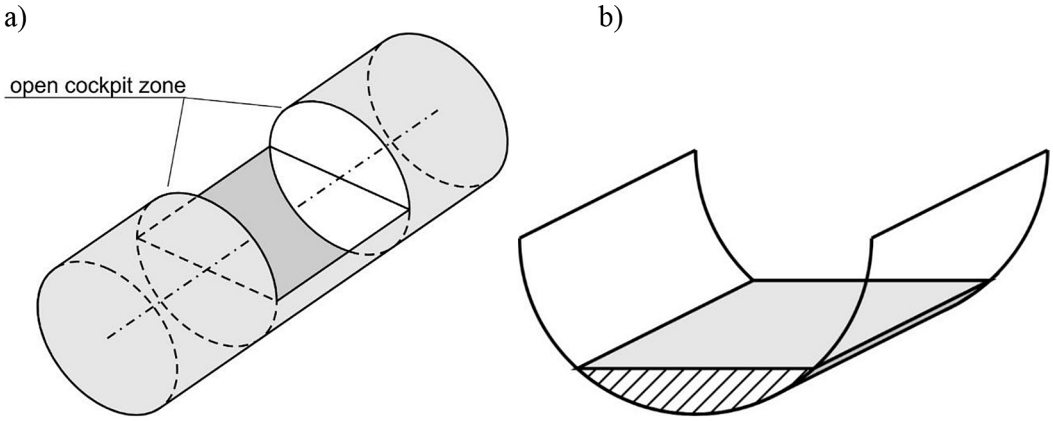

Figure 2. (a) The scheme of the cockpit cutout, (b) the example of the equivalent circumference

an additional structural component here. Commonly adopted solutions generally involve the use of framing, reinforcing trusses, or alternative, closed torsional circuits with small cross-sections, occupying a portion of the cockpit space (Fig. 2b). In the case of the latter, due to the small area of the Bredt field, the walls of the structure working in torsion must have significant thickness, leading to a relatively large increase in the overall mass of the construction.

The cockpit edge is the element most susceptible to stability loss. Because this is entirely unacceptable from the standpoint of requirements placed on the aircraft, it becomes necessary to also use reinforcements along the cutout edge, which in turn also leads to an increase in the aircraft's mass. Undesirable is also the local stability loss of covering segments bounded by skeletal elements, which, in the case of less critical construction zones, is permissible. In modern constructions, due to the increasingly common use of composites, a routine method of protecting the shell against stability loss has become the use of honeycomb sandwich structures. However, while they increase the levels of critical loads, they do not affect the increase in torsional stiffness of the shell. Research on various solutions of sandwich structures has been conducted in several scientific centers and aerospace manufacturers' research and development centers [1, 2].

In view of the above, it seems advisable to draw attention to an alternative solution, applied for example in the historical aircraft design of the PZL-37. The aircraft's wing was equipped with a torsion box, the creator of which was Prof. Franciszek Misztal. Hence, this type of box is commonly referred to as "Misztal's torsion box". The essence of the solution lies in the cooperation of an external smooth covering with a corrugated skin (Fig. 3). The external layer of the covering, serving aerodynamic functions, can have a relatively small thickness because the internal layer acts as a kind of spacer protecting the former from stability loss. The internal layer itself, due to its geometry, does not lose stability even at relatively high structural loads. An additional advantage of the solution is the presence of a series of closed circuits, represented by shaded areas. In the case of the torsion box, they contribute to increasing its torsional stiffness.

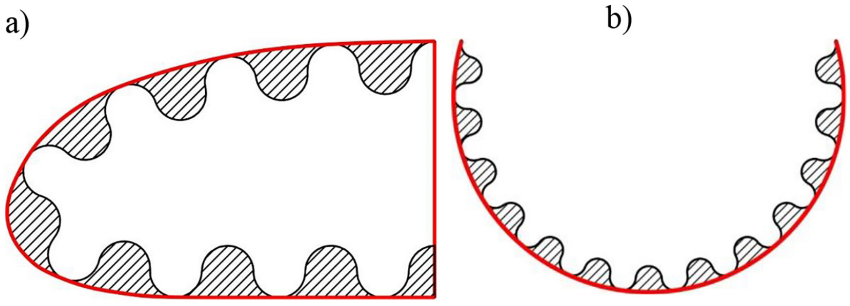

Figure 3. (a) The scheme of the „Misztal's torsion box", (b) application of the idea in open cockpit zone

To assess the suitability of using corrugated skin as a spacer, collaborating with a smooth skin, it is necessary to understand the susceptibility of this structure to stability loss. Several publications have addressed this issue [3–5].

A similar solution can be applied in the case of fuselage covering in the open cockpit area (Fig. 3b). In this case, the torsionally twisted outer circuit is open, and therefore practically lacks torsional stiffness. However, this stiffness can be provided by a series of closed circuits resulting from the presence of the inner layer. Additionally, as with the wing torsion box, the entire structure acts as a kind of sandwich structure, allowing for relatively small skin thicknesses, which facilitates meeting the required mass limits. Despite research efforts on the use of corrugated spacers in wing torsion boxes [6], or other closed-circuit structures [7], there appears to be a lack of publications on the considered problem. In this study, an attempt was made to conduct numerical experiments aimed at comparing various versions of the presented solution and their impact on the level of critical loads and torsional stiffness of the structure. A comparison was also made with a reference structure lacking the inner layer. The primary objective of the presented considerations was to determine the nature of the distribution of displacements and stresses in structures with a corrugated core and to compare them in different versions of the model. The benefits of using the proposed structural solution, in relation to the solutions routinely used in aviation engineering, were also demonstrated.

PURPOSE AND SCOPE OF THE STUDY

The subject of consideration was a thin-walled structure in the form of a cylinder segment, with an open circumference, consisting of a pair of ribs with a stretched covering between them (Fig. 4). The dimensions of the object were chosen with the next stage of research in mind, based on a model experiment, using the available experimental setup. It was assumed that models for experimental studies would be made using the additive manufacturing method,

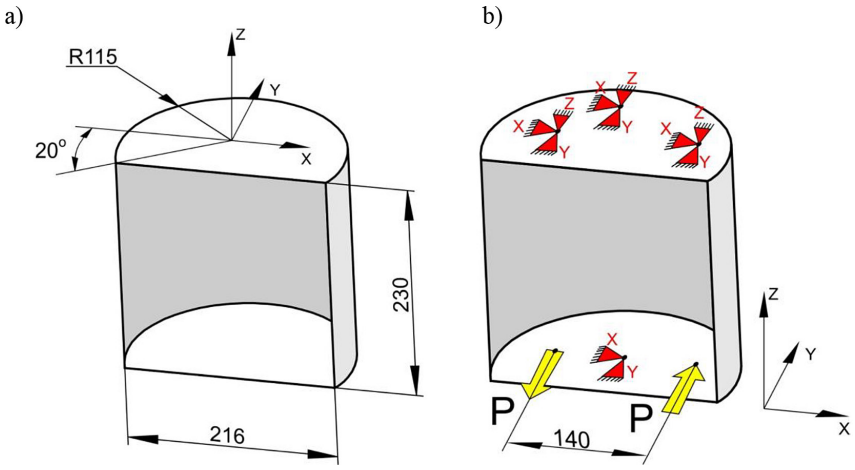

Figure 4. (a) Base geometry of the analysed structure [mm], (b) the diagram of the application of constraints and loading

thus, in numerical analyses, constant physical properties corresponding to the averaged values determined for polylactic acid (PLA) were applied. Although each of the printed layers exhibits orthotropy, the differences between the physical constant values for individual directions are relatively small, and in the case of several layers, they are difficult to determine. Therefore, due to the geometric complexity of some details of the analysed structures, a simplified, isotropic material model was adopted in the calculations.

Since the PLA polymer exhibits a relatively high range of elastic properties, physical nonlinearity was not considered in the calculations. Therefore, the calculations took the form of nonlinear analyses, taking into account geometric nonlinearity [8]. The mounting and loading diagram (Fig. 4b) corresponded to the requirements of the planned future model experiment and resulted from the design of the research setup. The upper rib was secured using screws, and the presence of a bearing was provided to enforce the torsion axis position. A series of versions of the structure were analysed. In all cases, the rib thickness was 6 mm, while the thickness of the covering was chosen so as not to cause changes in the total mass of the model. The following designations were adopted for further considerations:

- Version 1: reference model, devoid of reinforcements. The covering thickness was 1.6 mm,
- Version 2: model as in Version 1, equipped with stiffening framing,
- Version 3: model with multi-circuit reinforcement (Fig. 5a). The covering thickness was 0.6 mm,
- Version 4: model with multi-circuit stiffening and additional inner covering (Fig. 5b). The covering thickness was 0.4 mm.

From the perspective of thin-walled structure classification, versions 3 and 4 constitute sandwich structures. In most similar solutions used in aerospace engineering, the spacer function is performed by a so-called honeycomb core, which, however, does not bring the benefit of increasing the torsional stiffness of the system. The solutions presented above have the characteristics of spacers, effectively protecting the outer coverings from stability loss. Additionally, however, they represent a series of closed circuits, working on torsion. In Version 4, the use of an additional inner covering allows for a twofold increase in the number of these circuits. In the case of Version 3, the analyzed

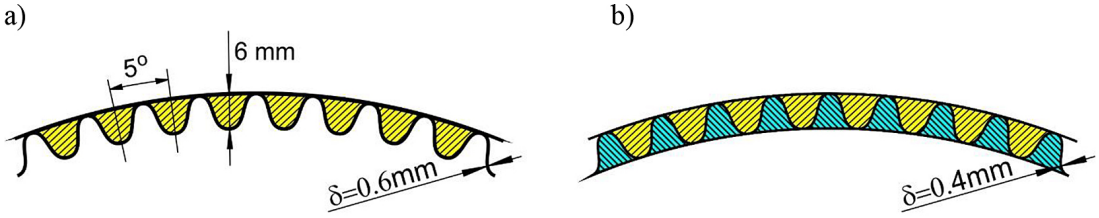

Figure 5. (a) Version 3, (b) Version 4

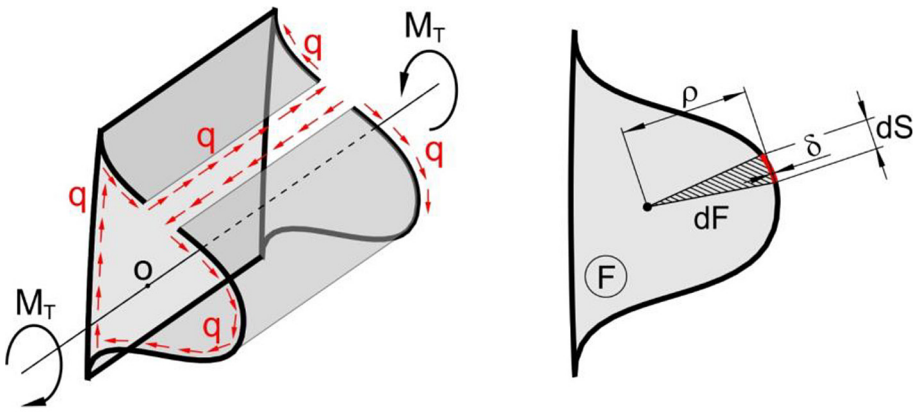

Figure 6. Statics of a single thin-walled torsion rod

structure can be treated as a series of interacting thin-walled rods. If the torsion of the structure is free, these systems are in a state of pure shear (Fig. 6). For a single rod, the following relation is valid [9]:

$$2qF = M_T \tag{1}$$

In the case of Version 3, the reinforcing structure consists of a series of thin-walled rods working independently (Fig. 7). In the Version 3 model, there are a total of 44 circuits, so for the complete structure, one can write:

$$88qF = M_{T_{TOTAL}} \tag{2}$$

On the other hand, the Version 4 model represents a multi-circuit thin-walled rod with a total of 87 circuits. Differences in mass flow rates appear in the shared walls of adjacent rods (Fig. 8). For the above system, the following relation is valid:

$$174qF = M_{T_{TOTAL}} \tag{3}$$

From the presented formulas, it follows that the values of flow rates in individual circuits decrease proportionally to the number of circuits, allowing for the use of proportionally reduced wall thicknesses while maintaining the unchanged mass of the structure. It is also worth noting that in the last of the solutions, the flow rates in the walls between adjacent circuits balance each other out. This means that the corrugated covering serves here as a spacer, unaffected by shape deformations.

The above simple analysis, conducted for the case of free torsion, allows for a preliminary estimation of the effectiveness of applying the considered solutions. However, considering the assumed nature of constraints and the static indeterminacy of the system, the most appropriate tool for conducting a comparative analysis of individual versions of the structure appears to be nonlinear FEM procedures.

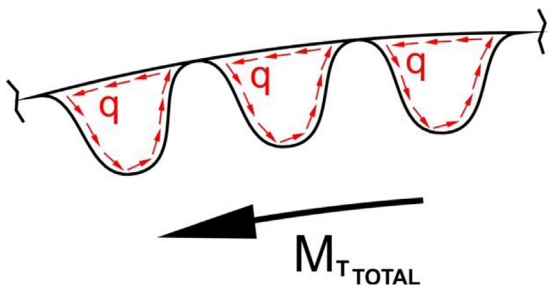

Figure 7. The schematic distribution of shear flow rates – Version 3

NUMERICAL ANALYSES

The nonlinear numerical analyses were conducted using MSC PATRAN/MARC software, based on the finite element method. The assumption of linearly elastic, isotropic material properties was adopted. The physical constants, determined in previously conducted experiments [10, 11], were: E = 3300 MPa, ν = 0.34. To compare results for different model versions, a force value of P = 800 N was used in all cases.

In its assumptions, a nonlinear analysis results in determining the equilibrium path of the system, constituting, in the general case, a hypersurface in a multi-dimensional state hyperspace [12, 13]. The number of dimensions corresponds to the total number of degrees of freedom of the system. The analysis is conducted in multiple stages. At each subsequent incremental step, associated with an increase in load, the discrete system satisfies the equation of residual forces:

$$r(u, \lambda) = 0 \tag{4}$$

where: u is the state vector, with components corresponding to the displacements of structural nodes in their current geometric configuration, λ represents the control parameter proportional to the load, and r is the residual vector containing unbalanced force components corresponding to the current state of deformation.

In all nonlinear procedures, there is an incremental phase, consisting of transitioning from state n to state n+1, during which the increments are not specified:

$$\Delta u_n = u_{n+1} - u_n, \Delta\lambda_n = \lambda_{n+1} - \lambda_n \tag{5}$$

In the case of incremental-correction procedures, there is an additional corrective phase allowing for the determination of the aforementioned quantities. It involves satisfying the system with the incremental control equation, also known as the constraint equation:

$$c(\Delta u_n, \Delta\lambda_n) = 0 \tag{6}$$

It represents a condition specified by the user, and its form arises from the applied correction strategy. In the case of the mentioned models, calculations were based on the Newton-Raphson method, with a load correction phase [14, 15]. In the first step of the calculation, it was performed for Version 1, which is the reference model without reinforcements (Fig. 9).

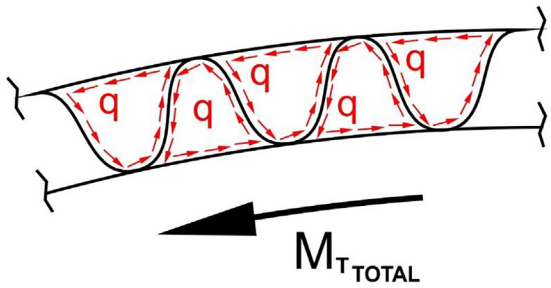

Figure 8. The schematic distribution of shear flow rates – Version 4

Table 1. Numerical models data

Model version	Number of nodes	Number of elements
Version 1	18049	17969
Version 2	19888	19850
Version 3	49996	54268
Version 4	49951	57472

The finite element mesh was based on four-node elements with bilinear shape functions. After a series of numerical experiments, the effective mesh density was determined. In all cases, the approximate side length of the element was 3 mm. The numbers of nodes and elements corresponding to each version are listed in Table 1. In each analysis, the loading and fastening model corresponded to the presented schematic (Fig. 4b). As a result of the numerical analysis of Version 1 model, distributions of resultant displacements were obtained (Fig. 10a), as well as stress distributions according to the von Mises hypothesis (Fig. 10b). The stress distribution indicates that the edges of the shell at the connections with the ribs are the most heavily loaded regions, resulting from a strong bending effect. On the other hand, the displacement distribution reveals the natural disadvantage of such structures, manifested as the

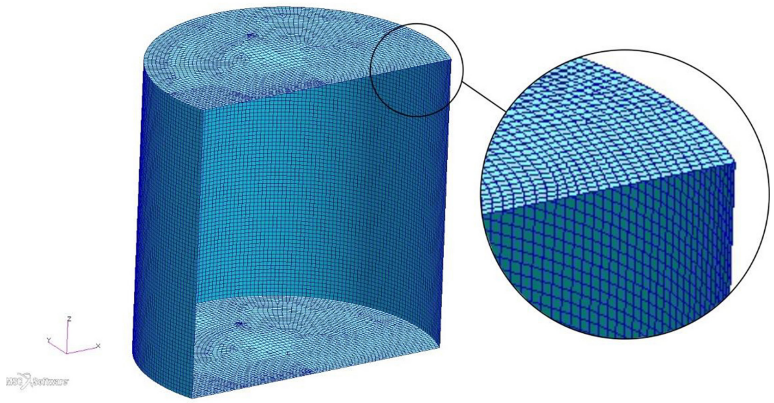

Figure 9. Finite elements mesh – Version 1

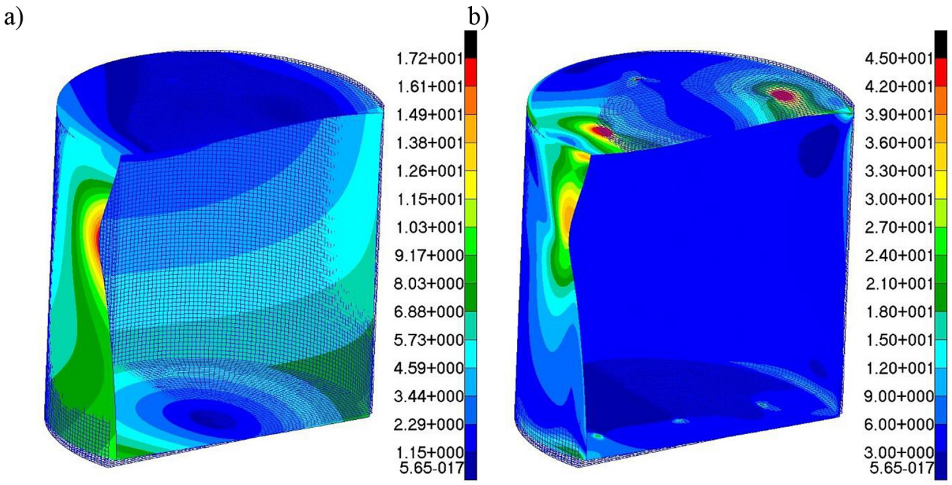

Figure 10. Version 1: (a) distribution of resultant displacements [mm], (b) effective stress distribution according to the von Mises hypothesis [MPa]

loss of stability of the free edge of the shell. This leads to a loss of stiffness along the edge and the emergence of strong stress concentrations in the buckling region. Such effects are unacceptable in aircraft constructions, necessitating the stiffening of the structure. As mentioned earlier, there are several possible variants of reinforcements. The simplest one appears to be reinforcing the critical area with framing. Such a solution is presented in Version 2 of the model (Fig. 11).

The additional component in the form of a reinforcing frame along the free edges of the structure in the analysed example had a thickness of 1.6 mm, corresponding to the thickness of the shell. Employing such a solution in each case entails an increase in the system's mass. This increase is dependent on the type and structure of the reinforcing element. Generally, relying on a relatively lightweight closing rib, as in the case of Version 2 of the model, does not solve the stability loss issue. This is evidenced by the result of the nonlinear analysis of the above model (Fig. 12). In this case, the area prone to stability loss is the edge of the frame. Due to the nature of the internal force distribution, the effective stress in the critical area reached a higher value than in the case of Version 1. Therefore, it is necessary to increase the thickness of the framing, which is associated with an increase in the mass of the structure. It is also important to emphasize that the cylindrical shell itself is a component of the considered structure prone to stability loss. Strengthening the framing contributes to increasing the level of critical load, but does not eliminate the structural problem associated with the mentioned phenomenon. In the next two versions of the analysed numerical model, solutions were included to stiffen both the shell itself, through the use of a spacer, and to reinforce its free edges (Fig. 13). The numerical analyses of the last two versions revealed the advantages of

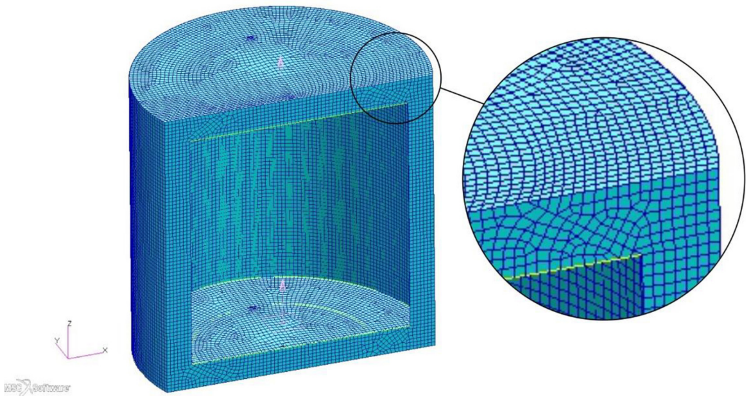

Figure 11. Finite elements mesh – Version 2

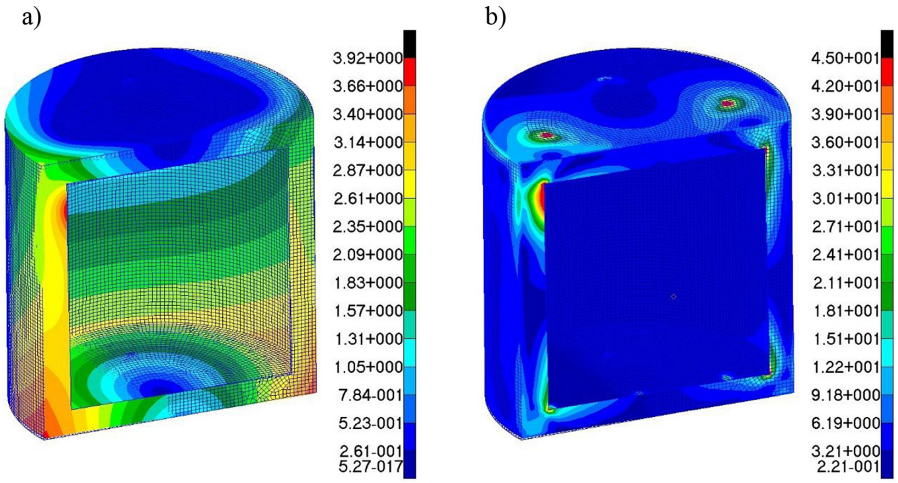

Figure 12. Version 2: (a) distribution of resultant displacements, (b) effective stress distribution according to the von Mises hypothesis

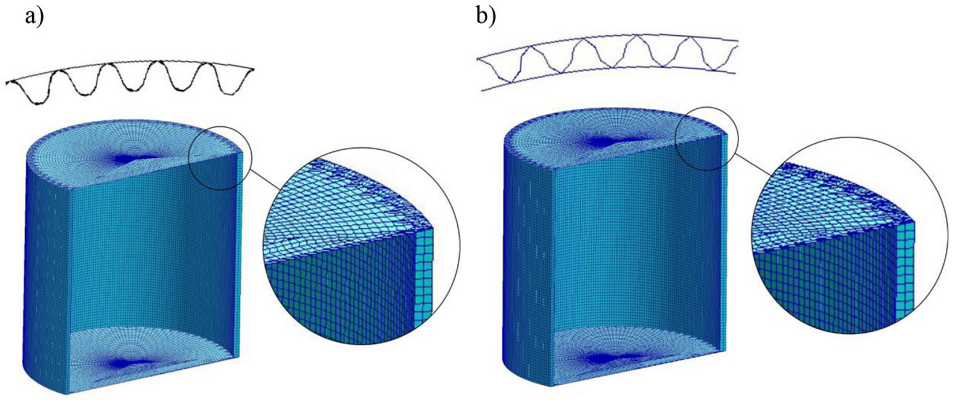

Figure 13. Finite element mesh: (a) Version 3, (b) Version 4

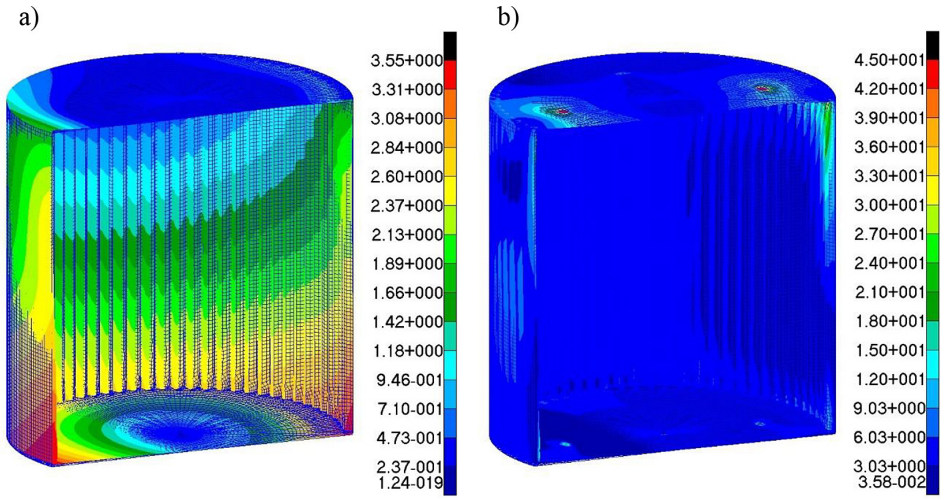

Figure 14. Version 3: (a) distribution of resultant displacements, (b) effective stress distribution according to the von Mises hypothesis

the proposed solutions. Despite the reduced thickness of the shells, allowing for the maintenance of unchanged structure mass, in both cases, the stability loss effect was eliminated (Fig. 14–15).

As indicated by the above calculation results, the distributions of effective stress and resultant displacements in the last two cases exhibit a high degree of similarity. This demonstrates the similar stiffness of the Version 3 and Version 4 models, as well as the high effectiveness of the analysed structures in transferring torsional loads. In both cases, stress concentrations of effective stress appear in the areas of the shell adjacent to the upper stringer. This is due to the fact that under the adopted boundary conditions, the dominant type of stress in these areas is normal stress, resulting from the constrained torsion of the structure.

Based on the results of nonlinear numerical analyses, a comparison of representative equilibrium paths was prepared, representing the relationships between the total twist angle and the total torsional moment (Fig. 16).

The above charts illustrate a significant difference in torsional stiffness between Version 1, without reinforcements, and the other versions. The characteristics corresponding to Versions 2, 3, and 4 practically overlap. Although in the case of Version 2, there is a loss of stability at the framing edge, resulting in a relatively small increase in the total twist angle. It is also important to note that the increase in stiffness of this version of the model was achieved with an increase in the structure's mass. In the case of Version 1, the buckling of the free edge of the shell results in slight nonlinearity in the graph.

The results of numerical analyses indicate that the use of an additional internal shell (Version 4) in the case of limiting the thickness of the shells to maintain the structure's mass does not significantly increase the effectiveness of the

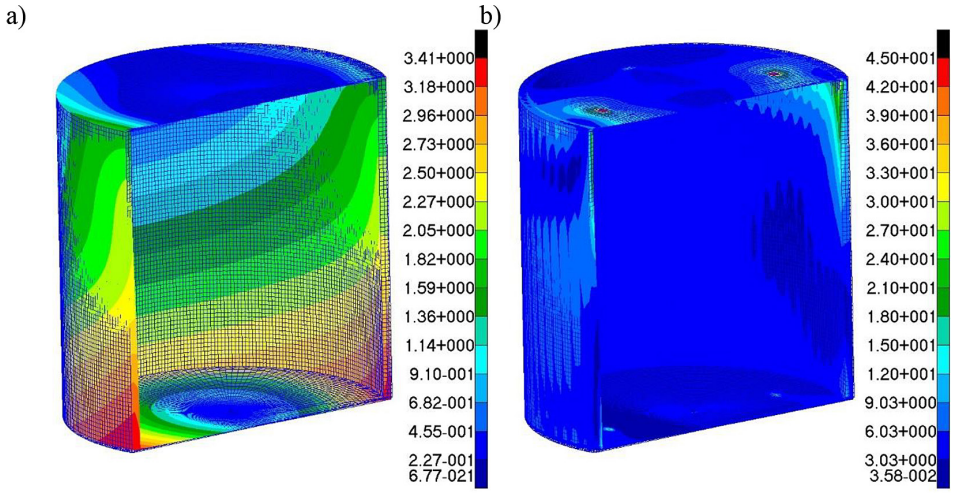

Figure 15. Version 4: (a) distribution of resultant displacements, (b) effective stress distribution according to the von Mises hypothesis

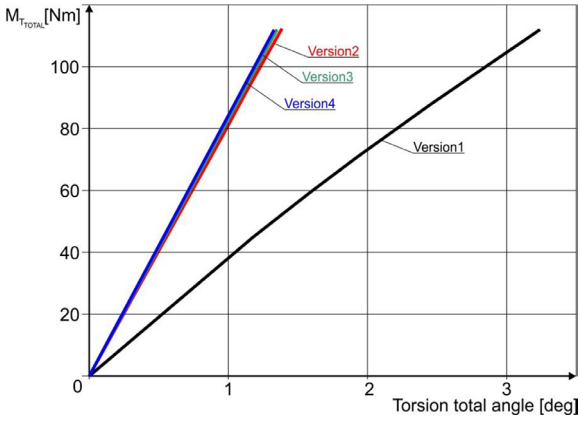

Figure 16. Representative equilibrium paths

solution. However, its presence may be crucial from a functional point of view. Considering that in such a case the tangential stresses in the walls of the spacer balance each other out, various options for selecting proportions between the thicknesses of the outer and inner shells, as well as the corrugated spacer itself, can be considered.

CONCLUSIONS

The considerations presented allow us to conclude that the analysed solutions for reinforcing open-sectioned twisted shells with corrugated spacers result in the desired increase in structural stiffness without the need for significant increases in mass, and they have a significant advantage over standard reinforcements such as frames or trusses. In the analysed case, approximately a twofold increase in the torsional stiffness of the structure was achieved compared to the reference variant, under non-free torsion conditions. The conducted numerical analyses included only one example of the geometric variant of the spacer. However, it should be emphasized that the selection of the radii of curvature of the sections of the corrugated shell depends on general design limits, especially the required effective cockpit volume. Using a thicker section of the spacer, associated with reducing its curvature, would result in an increase in the total surface area of the Bredt fields, thus increasing the torsional stiffness of the structure while simultaneously reducing the cockpit volume. It may also be worthwhile to consider various ways of shaping the cross-sectional profile of the spacer, particularly the selection of curvatures, as well as replacing them with variants of broken lines [16]. The selection of the most efficient solutions in terms of shaping the cross-section of the spacer may be the subject of separate considerations.

Due to the adopted boundary conditions and the presence of normal stresses, it would be worth considering the possibility of varying the thickness of the spacer along the axis of the structure. In the case of creating models for future experimental studies, additive manufacturing techniques appear to offer significant practical possibilities in this regard. However, such studies should be preceded by further numerical tests to eliminate ineffective variants of the considered structures.

The mentioned advantages of corrugated spacers suggest their superiority over honeycomb spacers in terms of resistance to shape deformations

under torsional conditions. This also suggests that similar solutions may have wide-ranging applications in structures other than open sections, particularly in the broader aerospace sector.

REFERENCES

1. Dayyani I., Shaw A.D., Saavedra Flores E.I., Friswell M.I., The mechanics of composite corrugated structures: A review with applications in morphing aircraft, Composite Structures1 December 2015.
2. Vinh T.L., Tailie J., Nam S.G., Mechanical behaviors and fracture mechanisms of CFRP sandwich composite structures with bio-inspired thin-walled corrugated cores, Aerospace Science and Technology 2022; 126: 10759.
3. Bo-Li Z., Wen-Hua B., Chen-Bao W., Jia-Qi Z., Hao-Jun S., Xiong W, Yan-Lin G., Experimental and numerical investigation into hysteretic performance of orthogonal double corrugated steel plate shear wall, Thin–Walled Structures 2024; 195: 111392.
4. Chen-Bao W., Bo-Li Z., Hao-Jun S., Yan-Lin G.,*, Wen-Jin Z., Li-Lan D., Global stability design of double corrugated steel plate shear walls under combined shear and compression loads, Thin–Walled Structures 2024; 199: 111789.
5. Ran D., Jun-De Y., Yu-Hang W., Qi-Qi L., Ji-Ke T., Cyclic shear performance of built-up double-corrugated steel plate shear walls: Experiment and simulation, Thin-Walled Structures 2022; 181: 110077.
6. Shaw A.D., Dayyani I., Friswell M.I., Optimisation of composite corrugated skins for buckling in morphing aircraft, Composite Structures 2015; 133: 358–380.
7. Dobrzański P., Czarnocki P., Lorenz Z., Shell structures – theory and application, CRC Press, 2013.
8. Kratochvíl J., Sadilek M., Musil V., Stančeková D., The effectiveness of strategies printing printer easy 3D maker, Advances in Science and Technology Research Journal 2018; 12(2): 197–205.
9. Kopecki H., Kopecki T., Święch Ł., Issues of aircraft structural strength, Rzeszów University of Technology Publishing House, Rzeszów, 2023.
10. Monaldo E., Ricci M., Marfia S., Mechanical properties of 3D printed polylactic acid elements: Experimental and numerical insights, Mechanics of Materials 2023; 177: 104551.
11. Kopecki T., Święch Ł., Experimental-numerical analysis of a flat plate subjected to shearing and manufactured by incremental techniques, Advances in Science and Technology Research Journal 2023; 17(4): 179–188.
12. Felippa C.A., Crivelli L.A., Haugen B., A survey of the core-congruential formulation for nonlinear finite element, Archives of Computer Methods in Engineering 1994; 1: 1–48.
13. Doyle J.F., Nonlinear analysis of thin-walled structures, Springer-Verlag, Luxemburg 2001.
14. Mazurek P., Fatigue strength of thin-walled rectangular elements in the state of post-critical deformation, Advances in Science and Technology Research Journal 2019; 13(2): 84–91.
15. Święch, Ł., Experimental and Numerical Studies of Low-Profile, Triangular Grid-Stiffened Plates Subjected to Shear Load in the Post-Critical States of Deformation, Materials 2019; 12: 3699.
16. Tewari K., Pandit M.K., Budarapu P.R., Natarajan S., Analysis of sandwich structures with corrugated and spiderweb-inspired cores for aerospace applications, Thin-Walled Structures 2022; 180: 109812.